

Impacts of 1.5 and 2 °C global warming on water availability and extreme hydrological events in Yiluo and Beijiang River catchments in China

Lülü Liu¹ · Hongmei Xu¹ · Yong Wang² · Tong Jiang^{1,3}

Received: 21 December 2016 / Accepted: 2 September 2017 / Published online: 23 September 2017
© The Author(s) 2017. This article is an open access publication

Abstract In the discussion of climate impacts, 1.5 and 2 °C have become iconic values. This study examines the impacts of 1.5 and 2 °C global warming on water availability, runoff seasonality, and extreme monthly and daily runoff in two catchments, using the semi-distributed hydrological model Hydrologiska Byråns Vattenbalansavdelning-D, based on a combination of five global climate models (GCMs) and four representative concentration pathways (RCPs). Subsequently, quantitative assessments were made for projection uncertainties from GCMs and RCPs. The two catchments are the Yiluo River catchment (YLC) in northern China and the Beijiang River catchment (BJC) in southern China. The results indicate wetter flood seasons for YLC and warmer mean annual temperatures, drier springs, and more severe floods over long return periods (25 and 50 years) for both catchments. The change magnitude of most indicators is expected to be larger in YLC than in BJC. Mean annual temperatures in both catchments are expected to have smaller changes under the 1.5 °C scenario than under the 2.0 °C scenario. However, the change magnitude of the other hydrological variables is projected to be approximately equivalent for both catchments under both scenarios. Uncertainties of projected impacts from GCMs are generally larger than those from RCP scenarios, for both catchments and warming scenarios, with the exception of mean annual temperature of BJC. These findings indicate that effective measures are required to

Electronic supplementary material The online version of this article (<https://doi.org/10.1007/s10584-017-2072-3>) contains supplementary material, which is available to authorized users.

✉ Hongmei Xu
xuhm@cma.gov.cn

✉ Tong Jiang
jiangtong@cma.gov.cn

¹ National Climate Center, China Meteorological Administration, Beijing 100081, China

² Chongqing Climate Center, Chongqing 401147, China

³ Collaborative Innovation Center on Forecast and Evaluation of Meteorological Disasters, School of Geography and Remote Sensing, Nanjing University of Information Science & Technology, Nanjing 210044, China

address increasing annual temperatures, more severe flood events (25- and 50-year return periods), and drier spring seasons in both catchments and wetter flood seasons in YLC.

1 Introduction

The global mean surface temperature (GMT) has increased 0.85 °C over the period 1880–2012 and will likely increase by 0.3 to 0.7 °C in the near term. As the planet continues to warm, the numbers of cold days and nights have decreased while the numbers of warm days and nights have increased globally since about 1950 (IPCC 2013). Climate change will likely amplify climate-related risks and create new risks for natural and human systems (IPCC 2014a). The impact of climate change on people's livelihoods in certain regions could be catastrophic and is therefore of considerable concern to policy makers. For example, extreme flood events have increased substantially in the Pearl River basin since 1980 (Wu et al. 2013), and more frequent and severe intrusions of saltwater into the Pearl River delta have occurred since 1990 (You et al. 2006).

Among the 200 top largest ocean-reaching rivers worldwide, 15 and 19 showed statistically significant downward and upward trends in annual runoff, respectively, during 1948–2004 (Dai et al. 2009). In China, significant decreases in annual runoff of the Yellow River and upper reaches of the Yangtze River over 1950–2008 have been detected (Wang et al. 2013). A large number of studies have assessed impacts of climate on water resources at either global or regional scale under different emission scenarios using various global climate models (GCMs). Results have been reported in a series of assessments by the IPCC (2014b) and in other publications (Dankers et al. 2014; Liu et al. 2013a; Todd et al. 2011; Schewe et al. 2014). The percentage of the global population that has experienced water scarcity and major river flooding is projected to increase with increased warming in the twenty-first century (IPCC 2014a).

Recent climate change has had widespread impacts on natural and human systems, and warming caused by continued emission of greenhouse gases will increase the risk to people and ecosystems (IPCC 2014c). In the 2010 Cancún Agreement (UNFCCC 2010), the signers agreed that global warming should be restricted to no more than 2 °C above pre-industrial levels. The 2015 Paris Agreement (UNFCCC 2015) marked another step forward and included a twofold temperature goal of “holding the increase in the global average temperature to well below 2 °C above pre-industrial and pursuing efforts to limit the temperature increase to 1.5 °C”. The 1.5 °C threshold was included because a number of regions may face high risks under a 2 °C increase (e.g., Schewe et al. 2011). Accordingly, the 1.5 and 2 °C thresholds have become a staple of climate change discussions.

Climate impacts and risks at various global mean temperature increases have been examined in previous studies. For example, the risk to human support systems because of increase in extreme rainfall and drought is expected to be much higher under a 4 °C increase than a 2 °C increase (Schellnhuber et al. 2012). Virtually all tropical coral reefs are projected to be at risk of severe degradation under a 2 °C warming scenario; this percentage is projected to decline to 70% by 2100 under a 1.5 °C scenario (Schleussner et al. 2016). However, a comprehensive study is needed of the difference in climate impacts at the 1.5 and 2 °C levels. The assessment of climate change impacts is important for policy makers to make mitigation efforts.

To identify potential threats from global warming, this study investigates the impacts of climate change on water availability and extreme runoff in the Yiluo River catchment (YLC) in northern China and in the Beijiang River catchment (BJC) in southern China under global

warming of 1.5 and 2 °C. In general, global and catchment hydrological models are applicable to estimate hydrological impacts. However, climate impacts vary regionally, and adaptation policies are implemented at the regional scale. To provide reliable information for regional stakeholders and tailored adaptation policies, we used one validated hydrological model, considering that catchment hydrological models usually have more explicit representation of catchment water resources than global models (Gosling et al. 2011).

We first considered relative change against the baseline in projected temperature and precipitation at annual and monthly scales under global warming of 1.5 and 2 °C. Then, we investigated changes in simulated annual mean and seasonal runoff as well as extreme monthly and daily runoff, based on a simulation using the hydrological model Hydrologiska Byråns Vattenbalansavdelning (HBV)-D under four representative concentration pathway (RCP) scenarios and five GCMs. Finally, uncertainties inherent in GCM structures and RCP scenarios were quantitatively investigated.

2 Study area and datasets

2.1 Study basin description

YLC (Fig. 1) (33.5°–35° N, 109.5°–113° E) flows into the middle reaches of the Yellow River in northern China, has a drainage basin of 18,881 km², and had a population of 7.7 million in 2010 (Fu et al. 2014). The Heishiguan hydrological station is where the river joins the main stream of the Yellow River, and the control watershed area is 18,563 km² (He et al. 2007). Mountainous and hilly areas, loess, and [alluvial plain](#) (valley) cover 52.4, 39.7, and 7.9% of the catchment, respectively (Wang and Qian 2012). The catchment has a semi-humid climate, and the annual average mean temperature is between 10 and 13 °C. The maximum monthly mean temperature varies from 17 to 20 °C, and the minimum monthly temperature from 5 to 7 °C (Liu et al. 2013b). The mean annual precipitation of ~ 660 mm is not evenly distributed throughout the year. Because of the East Asian summer monsoon, precipitation during the flood season (June to September) accounts for 60% of the annual total (He et al. 2007). Thus, the flood risk is the highest in summer, which is one of the reasons for seasonal variation in runoff. The annual runoff is ~ 2.74 million m³ (Wang and Qian 2012). Runoff levels correspond to the seasonal precipitation pattern. Runoff during the flood season accounts for ~ 46.5% of the annual total, whereas that from January to April represents only 17.1% (Guo and Zhao 2015). Natural stream flow has been disturbed by reservoir operation, lift irrigation, and soil and water conservation since 1970, especially by a decline in cultivated land area and increase of urban industrial land area since 1990 (Li et al. 2015). However, 80% of annual runoff is driven by precipitation (Zhao et al. 2006).

BJC (Fig. 1) (23.1°–25.5° N, 111.9°–114.8° E) is the second largest tributary of the Pearl River in southern China, has a drainage basin of 52,068 km² (He and Chen 2003), and had a population of 8 million in 2010 (Fu et al. 2014). The upper Shijiao station area makes up 82.1% of BJC. In the upper area of the station, a reservoir with total capacity 1.9 billion m³ began operation in 1999 to prevent floods (Huang et al. 2015). BJC has humid climate conditions influenced by the subtropical monsoon. Annual mean temperature is between 18 and 21 °C, and the maximum monthly temperature is in July or August (Gao et al. 2016). Mean annual precipitation varies from 712 to 4040 mm (Wang 2014); 75% of annual precipitation falls during flood season (April through September), whereas only 5.9% falls

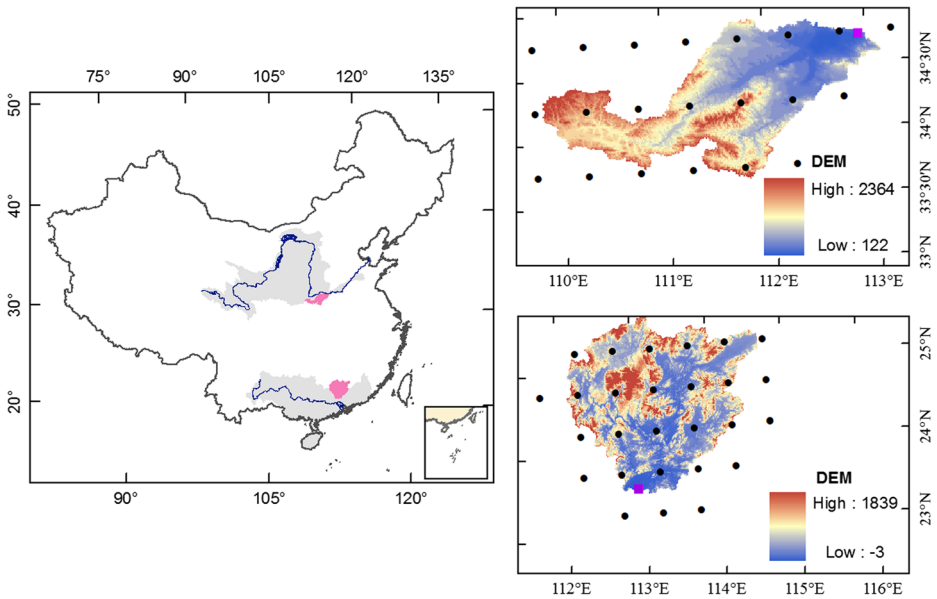


Fig. 1 Overview map of YLC (upper right panel) in the Yellow River basin of northern China and BJC (lower right panel) in the Pearl River basin of southern China, with grid notes of climate forcing (dots) and hydrological stations (squares)

from November to January (He and Chen 2003). Mean annual runoff is 42.8 billion m^3 . This runoff is modulated by the seasonal precipitation pattern, with 70–80% of the annual total occurring in the flood season (Huang et al. 2015). The early flood season (April to June) is mainly influenced by frontal rainfall, and the late flood season (July to September) is characterized by tropical cyclones. Most floods are during the early flood season (Gao et al. 2016). Studies have indicated that the rainfall–runoff relationship has been altered since 1973, primarily by urbanization and soil erosion. However, it has been indicated that the impact of such human activities is much smaller than changes in annual runoff (Li and Zhang 2014).

2.2 Available data

Digital elevation model (DEM), land use, and soil data were used in the study. A DEM with scale 1:250,000 was developed by the National Geomatics Center of China (Shang et al. 2004). Soil field capacity was estimated based on soil property data from the FAO Soil Map of the World (FAO 1995–2003). Digital land use map at scale 1:500,000 was developed by the Ministry of Land and Resources of China (Zha et al. 2001). Because of data availability in the future, changes in land use were not incorporated.

Daily temperature and precipitation at $0.5^\circ \times 0.5^\circ$ resolution during 1958–2001 were derived from the Water and Global Change Program (WATCH) meteorological forcing datasets (WFD) (Weedon et al. 2010), and they were used as climate forcing to calibrate and validate the hydrological model in our study. Although a newer WFDEI dataset (Weedon et al. 2014) can improve variables such as radiative fluxes as compared with the WFD, the WFD is acceptable here because only temperature and precipitation were used.

Climate projection information from five GCMs (GFDL-ESM2M, HaDGem2, IPSL_CM5A_LR, MIROC-ESM-CHEM, and NorESM1-M) was derived from the Inter-Sectoral Impact Model Inter-comparison Project (ISI-MIP). These models were selected to span GMT change and relative precipitation change as effectively as possible (Warszawski et al. 2014). Climate outputs were spatially interpolated into $0.5^\circ \times 0.5^\circ$ resolution and corrected using a trend-preserving bias correction approach (Hempel et al. 2013), with coverage of the period 1950 to 2099.

The digital monthly runoff records during 1970–2000 at the Heishiguan hydrological station along the Yiluo River were provided by the Yellow River Resources Bureau, and records at the Shijiao station along the Beijiang River were provided by the Pearl River Resources Bureau. They were used to calibrate and validate the HBV model for the two catchments.

3 Methodology

3.1 Climate change scenarios

The future time horizon of 1.5 and 2 °C global warming was derived based on a 30-year running mean of GMT for each of the 20 combinations of four RCPs (RCP2.6, RCP4.5, RCP6.0, and RCP8.5) and five GCMs. When the GMT anomaly of the 30-year running mean relative to pre-industrial level reaches the 1.5 or 2 °C thresholds, the 30-year window is sampled as the corresponding time horizon of the global warming scenario. Among the 20 combinations, 16 scenarios show mean GMT increases exceeding the threshold of 2 °C above pre-industrial level, and 18 scenarios exceed the threshold of 1.5 °C. The changes in projected variables for the two catchments are quantified relative to the reference period (1976–2005).

3.2 Hydrological model: HBV-D

In various versions, the HBV model has been used under a wide range of climatic and physiographic conditions, from small watersheds to large basins in more than 40 countries (Graham and Bergström 2001; Kang et al. 2001; Lindström et al. 1997; Xu 2009; Zhao et al. 2007). Derived from the “Nordic” HBV model (Saelthun 1996), the HBV-D model (Krysanova et al. 1999) divides a basin into smaller hydrological units by parameters that include elevation, land cover type, and climate conditions. These units allow better representation of local characteristics and consequently improve model performance. Therefore, compared with the original HBV model, HBV-D is considered more appropriate for investigating hydrological impacts of global climate change on large basins (Krysanova et al. 1999). The model has also been used in China to simulate runoff of the Pearl (Liu et al. 2013a) and Yangtze (Su et al. 2017) rivers and define rainfall thresholds for river flood warning for many catchments and various climate conditions nationwide (Fan et al. 2014; Meng et al. 2015; Zhang et al. 2014; Zhao et al. 2015).

3.3 Calibration and validation of hydrological model

Observed monthly runoff during 1970–2000 was used to calibrate and validate the HBV model. Because natural hydrology in the two study catchments has been disturbed by human

activities in nearly every year of that period, it is difficult to recreate undisturbed conditions, and the human alternations of the natural stream flow are not accounted in the hydrological model. The performance of HBV was evaluated using the following criteria: Nash–Sutcliffe efficiency (Ens) (Nash and Sutcliffe 1970), coefficient of determination (R^2), and water balance error (WBE). In general, a hydrological model can effectively simulate stream flow for a given basin if Ens and R^2 are > 0.50 .

$$Ens = 1 - \frac{\sum_{i=1}^n (Q_{obs,i} - Q_{sim,i})^2}{\sum_{i=1}^n (Q_{obs,i} - \bar{Q}_{obs})^2} \quad (1)$$

$$R^2 = \frac{\left[\sum_{i=1}^n (Q_{obs,i} - \bar{Q}_{obs}) (Q_{sim,i} - \bar{Q}_{sim}) \right]^2}{\sum_{i=1}^n (Q_{obs,i} - \bar{Q}_{obs})^2 \sum_{i=1}^n (Q_{sim,i} - \bar{Q}_{sim})^2} \quad (2)$$

$$WBE = 100 \times \frac{\sum_{i=1}^n Q_{sim,i} - \sum_{i=1}^n Q_{obs,i}}{\sum_{i=1}^n Q_{obs,i}} \quad (3)$$

where Q_{sim} and Q_{obs} are the simulated and observed monthly runoff, respectively; \bar{Q} is the mean monthly runoff; i is the month; and n is the length of the monthly runoff series for the calibration or validation period.

Monthly and seasonal patterns of observed monthly runoff were acceptably reproduced as shown in Fig. 2a, with bias (quantified by WBE) of 11 and 15% for YLC for the calibration (1970–1980) and validation (1981–2000) periods, respectively. For the two periods, Ens is 0.73 and 0.73, and R^2 is 0.86 and 0.88, respectively. For BJC, the observed monthly runoff was reproduced well (Fig. 2b), with bias = -1% and 5%, $Ens = 0.90$ and 0.83, and $R^2 = 0.96$ and 0.93 for the calibration and validation periods, respectively. These results show that the model is capable of sufficiently accurate simulations of long-term runoff, although runoff was overestimated during 1991–2000 for YLC. This is partially because of the Guxian Reservoir operation since 1994, decline of cultivated land area, and increased urban industrial land area since 1990 (Li et al. 2015).

The satisfactory performance for the calibration and validation periods together with the successful application of HBV-D to different climate regions ensures that the model could be used to project the impacts of climate change on river runoff in our study under current human activities.

3.4 Hydrological projections and uncertainty

Mean annual, mean monthly, and extreme runoff at monthly and daily scales were calculated to investigate various hydrological responses of the two catchments under 1.5 and 2 °C global warming scenarios. The extreme (high and low) monthly runoff is expressed by Q5 (high flow) and Q95 (low flow), for which the monthly runoff exceeded 5 and 95% of the time, respectively. The extreme daily runoff is expressed by POT3, which represents the maximum peaks sampled at an average rate of three events per year using standard independence criteria (Bayliss and Jones 1992; Kay et al. 2009). To facilitate inter-model comparison, the percentage

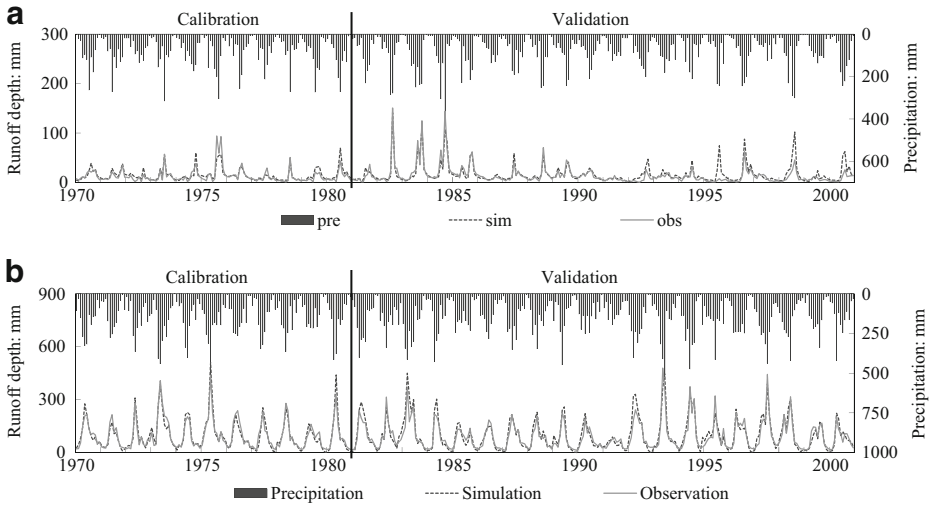


Fig. 2 Monthly precipitation and observed/simulated runoff at the Heishiguan station along Yiluo River (a) and Shijiao station along Beijing River (b) for periods of calibration (1970–1980) and validation (1981–2000)

changes in annual runoff, Q95, Q5, and POT3 were compared with the baseline period. However, changes in monthly runoff are expressed as percentage anomalies of annual runoff. The uncertainty envelope of climate projection is shown as a function of each GCM-RCP combination under the assumption that each scenario had an equal probability of occurrence.

The uncertainty of GCM structure was estimated using standard deviation of the mean of all RCPs under 1.5 and 2 °C warming, respectively, whereas the uncertainty of RCP scenarios was estimated using standard deviation of the mean of all GCMs under each global scenario.

4 Results

4.1 Annual temperature and precipitation

In YLC annual mean temperature is expected to increase by 1.4 and 2.1 °C in response to the 1.5 and 2 °C warming scenarios, respectively (Fig. 3a). Mean annual precipitation will decrease by 2% under 1.5 °C warming and increase by 2% under 2.0 °C warming (Fig. 3c). The direction and magnitude of changes vary with the RCP-GCM combination. Additional scenarios show a decrease under 1.5 °C warming and an increase under 2 °C warming. The uncertainty from GCMs is larger than that from RCPs, for both projected average annual temperature and annual precipitation. The uncertainty from GCMs is one to six times that from the RCPs for projected average annual temperature and approximately two times for annual precipitation.

In BJC, the projected mean temperature increases are 1.2 and 1.8 °C (Fig. 3b), respectively. The uncertainties from GCMs and RCPs are comparable. Only a slight change in mean annual precipitation is projected, although predictions of the GCMs and RCPs present wide variations (Fig. 3d). The uncertainties from GCMs are four and six times that from RCPs under the 1.5 and 2 °C global warming scenarios, respectively.

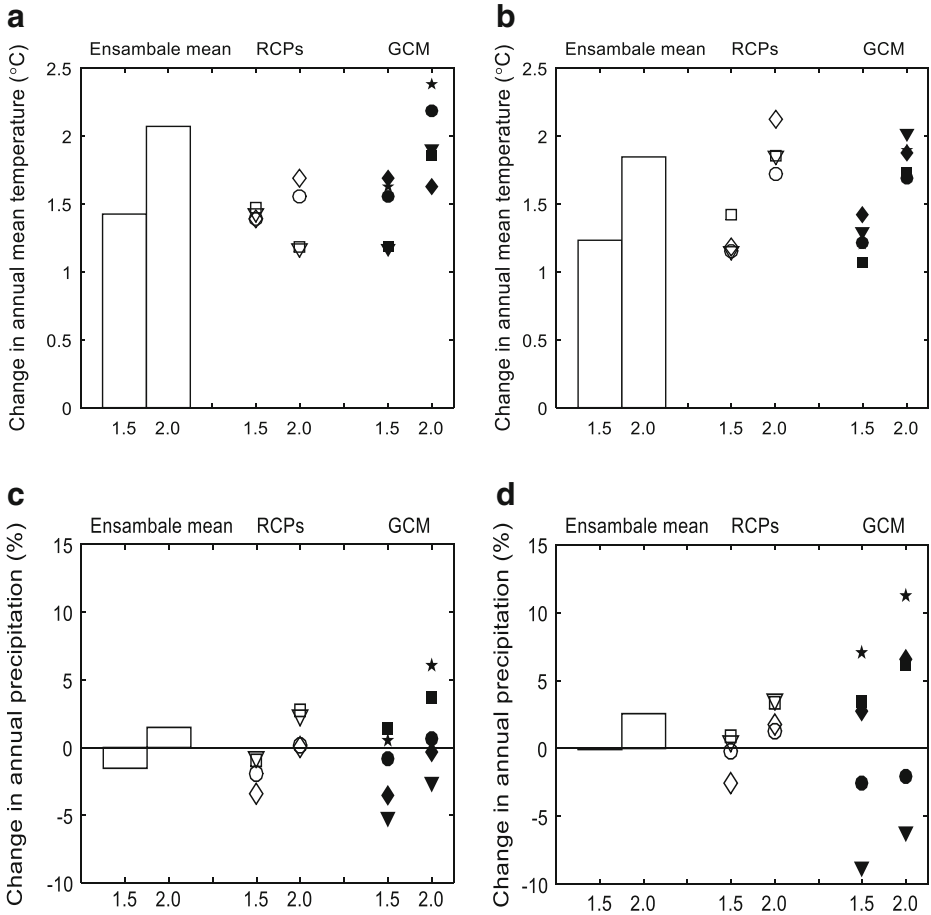


Fig. 3 Changes in annual mean temperature for YLC (a) and BJC (b) and percentage changes in annual precipitation for YLC (c) and BJC (d) relative to the reference period (1976–2005) under 1.5 and 2 °C global warming scenarios (Columns represent the projected mean of all combination of GCMs and RCPs. Hollow diamond, square, circle, and triangle represent RCP2.6, RCP4.5, RCP6.0, and RCP8.5 respectively. Solid diamond, square, circle, triangle, and pentagram represent GFDL-ESM2M, HaDGem2, IPSL_CM5A-LR, MIROC-ESM-CHEM, and NorESM1-M climate models respectively.)

As illustrated in Fig. 3, a spatiotemporal discrepancy of changes in annual precipitation was projected between the two catchments and two scenarios. This may be partially explained by the time-varying change in precipitation. In the two catchments, the projected time to reach threshold 2 °C is later than that to reach 1.5 °C (Table S1), and interdecadal oscillation has been detected (Hao et al. 2007; Lu et al. 2013). However, it may also be explained by strong regional-scale spatial heterogeneity in the simulated precipitation, because surface fields such as topography, coastlines, and vegetation are linked to climate models (IPCC 2013).

4.2 Annual mean and seasonal runoff

For YLC in northern China, the projected mean annual runoff will decrease by 22% compared with that of the baseline period for the 1.5 °C global warming scenario and by 21% for the

2 °C warming scenario (Fig. 4a). The uncertainty from GCMs is larger than that from RCPs, and the former is more than twice the latter under the 1.5 and 2 °C global warming scenarios.

As shown in Fig. 4c, the monthly percentage of annual runoff is projected to decrease during the first 6 months of a year, especially in April and May, when the runoff is expected to decrease by 3 and 4%, respectively. However, the runoff will increase during the second half of a year (i.e., by 2 and 4% in September and October, respectively). These shifts will lead to changes in seasonality. The catchment will experience drier springs but wetter flood seasons. However, in most months, the additional 0.5 °C increase in global temperature (from 1.5 to 2 °C) does not correspond to a considerable difference in runoff. Furthermore, the direction and magnitude of the projected changes in monthly runoff are constrained by the GCMs and RCPs. The 12-month average uncertainty from GCMs is four times that from RCPs under the 1.5 °C global warming scenario, but no more than twice that under the 2 °C scenario.

For BJC, mean annual runoff is projected to increase by less than 1 and 3% compared with that during the baseline period for the 1.5 and 2 °C global warming scenarios, respectively. The directions and magnitudes vary with RCP and GCM (Fig. 4b). The uncertainties from GCMs are two and three times that from RCPs under the 1.5 and 2 °C warming scenarios, respectively.

The mean monthly percentage of annual runoff during spring (March–May) is projected to decrease by 1 to 2%, with smaller changes under warming of 1.5 °C than 2 °C (Fig. 4d). These changes will cause a drier early flood season. However, in other months, the proportions of

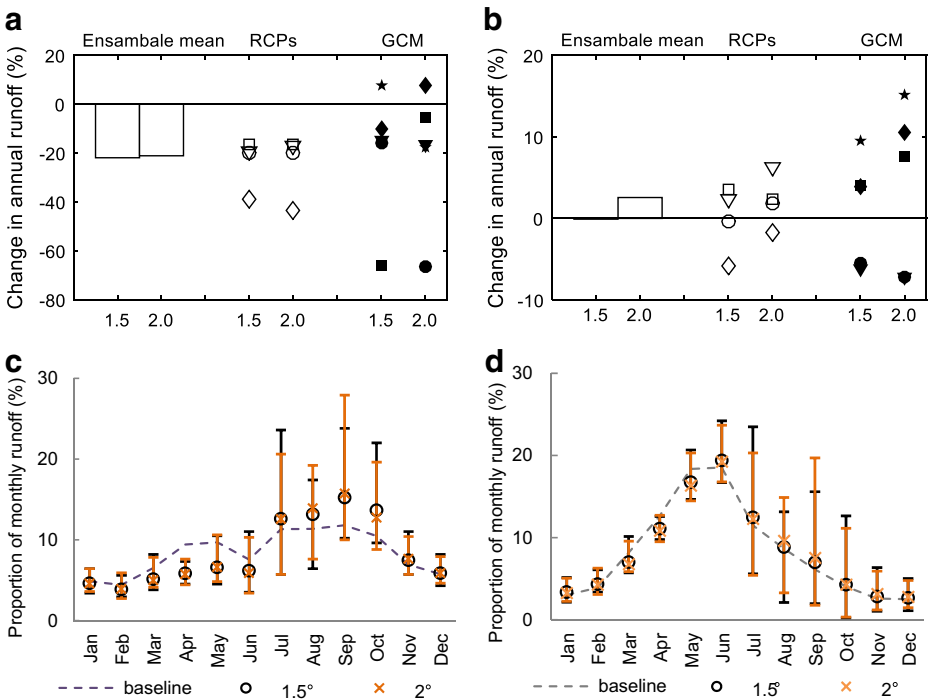


Fig. 4 Percentage changes in annual runoff relative to the reference period (1976–2005) for YLC (a) and BJC (b) and proportion of monthly runoff in annual runoff for YLC (c) and BJC (d) under 1.5 and 2 °C global warming scenarios (The meaning of symbols in Fig. 4a and b is the same as that in Fig. 3. Bars in Fig.4c and d show the maximum and minimum values of all projected hydrological scenarios.)

annual runoff will increase with smaller amplitudes. The importance order of uncertainty from GCMs and RCPs is consistent with that for YLC, and the 12-month average uncertainty from GCMs is twice that from RCPs.

4.3 Extreme monthly runoff

For YLC, the mean Q95 is projected to decrease by 31 and 29%, and the mean Q5 is projected to decrease by approximately 5 and 1% under the 1.5 and 2 °C global warming scenarios, respectively (Fig. 5a). Projected mean changes in extreme runoff are slightly smaller under the 2 °C scenario than under the 1.5 °C scenario. A projected significant decline in low runoff indicates an increased possibility of dry seasons getting drier under warming of 1.5 and 2 °C, as suggested in the Sect. 3.2. The mean high runoff will decrease, although based on the projection uncertainties, that runoff is still likely to increase under certain scenarios (Fig. 5c). The uncertainty from GCMs is 1.6–3.9 times greater than that from RCPs.

For BJC, the mean Q95 is projected to decrease by 2% under 1.5 °C warming and decrease by 1% under 2 °C (Fig. 5b). However, the mean Q5 is expected to have a much weaker change. Compared with YLC, changes in the two extreme events are smaller (see projected directions and amplitudes of changes in extreme monthly runoff in Fig. 5d). The uncertainty from GCMs is 1.4 to 5.5 times greater than that from RCPs.

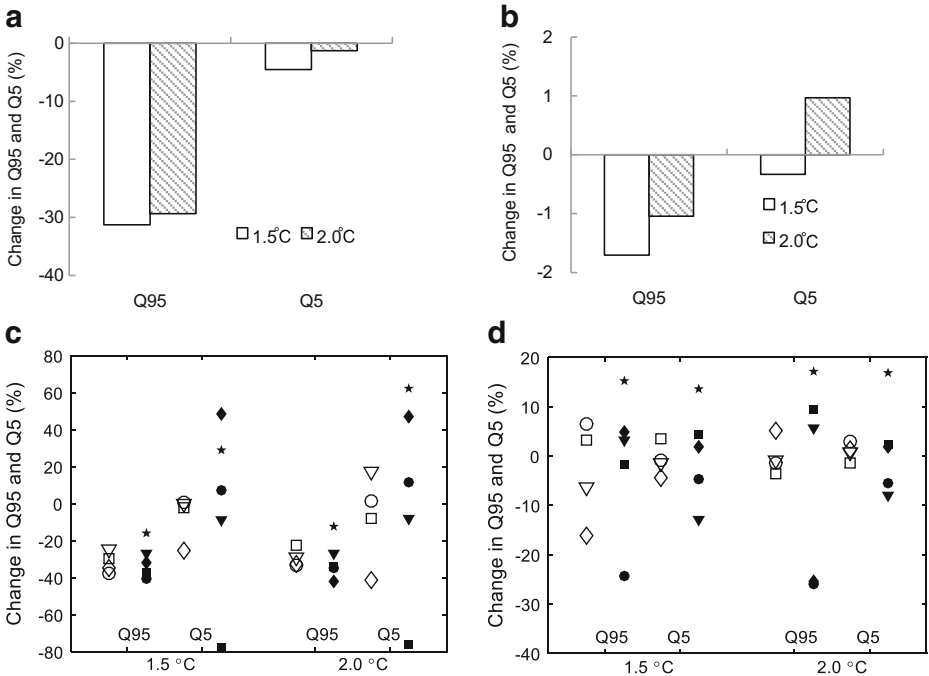


Fig. 5 Percentage changes in Q5 and Q95 monthly runoff relative to the reference period (1976–2005) for YLC (a) and BJC (b) rivers and uncertainties from RCPs and GCMs for YLC (c) and BJC (d) under 1.5 and 2 °C global warming scenarios (The meaning of symbols is same as that in Fig. 3.)

4.4 Floods

For YLC, under the 1.5 and 2 °C global warming scenarios, mean POT3s are projected to decrease by 8 and 10% for a 5-year return period, respectively, but expected to increase by 13 and 11% for a 25-year period and 27 and 27% for a 50-year period (Fig. 6a). These findings indicate that more severe floods will occur infrequently, that less severe floods will be more frequent, and that change magnitudes for long return periods will be larger than those for short return periods. However, the difference in change magnitude between the 1.5 and 2 °C global warming scenarios is insignificant. The uncertainty from GCMs is one to three times that from RCPs for the return periods mentioned above.

A similar pattern is projected for BJC, with more severe floods occurring infrequently, and an insignificant projected difference between the 1.5 and 2 °C global warming scenarios. Specifically, in response to those two scenarios, mean POT3s are projected to increase by 6 and 6% for a 25-year return period, by 9 and 10% for a 50-year period, and by < 1% for a 5-year period, respectively (Fig. 6b). Uncertainties from GCMs are one to five times greater than those from RCPs.

5 Conclusions and discussion

The present study revealed the probability of warmer annual temperatures, decreases in monthly runoff in the first half-year but increases in runoff in the last half-year, heavier floods over long return periods (25 and 50 years), and greater changes in Q95 than in Q5 monthly runoff for both catchments under 1.5 and 2 °C global warming.

The results indicate that global warming could have different climatic and hydrologic impacts on the two catchments in northern and southern China. Specifically, the mean annual temperature projection indicates a greater temperature increase for YLC than BJC under both global warming scenarios. The mean annual runoff and monthly low runoff projections suggest that compared with the baseline, YLC catchment may become drier but that of BJC would have normal annual runoff and only slightly reduced low runoff. YLC is also projected to have more significant changes in flood patterns over 25- and 50-year return periods than BJC.

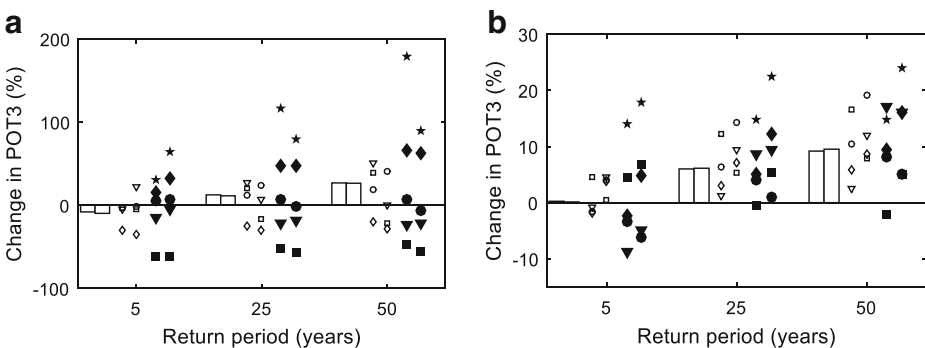


Fig. 6 Percentage changes in POT3 for return periods 5, 25, and 50 years relative to the reference period (1976–2005) and uncertainties from RCPs and GCMs for YLC (a) and BJC (b) under 1.5 and 2 °C global warming scenarios. (The meaning of symbols is same as that in Fig. 3. Two neighboring same symbols indicate global warming 1.5 and 2 °C, respectively)

Annual temperature would rise in response to both global warming scenarios, with a smaller change magnitude under the 1.5 °C scenario than the 2 °C scenario for both catchments. However, the projected magnitude of changes in flood pattern is roughly the same under both scenarios. For YLC, most scenarios show a decrease in annual precipitation under the 1.5 °C scenario and an increase in that precipitation under 2 °C warming. For BJC, the projection of mean annual runoff and monthly high and low runoff shows minor changes for both warming levels.

The present findings have implications for water resource management. The study identifies potential threats from global warming. For example, both catchments may experience warmer annual temperatures and more severe floods with long-term return periods, and YLC in northern China may have drier springs and early summers (March–June) but wetter mid-summers to mid-autumns (July–October). Thus, the results indicate that effective water management measures must be developed. However, there were slight changes in annual runoff projected against the baseline. BJC in southern China may benefit from 1.5 and 2 °C global warming because of runoff declines during April–May, which would potentially lead to fewer floods during early flood season (Gao et al. 2016).

Our uncertainty analysis shows that for both catchments, projection uncertainties for most indicators from GCMs are larger than those from RCP scenarios, with the exception of annual temperature of BJC. However, the uncertainties calculated here are not fully representative. Certain uncertainty sources were not investigated, such as hydrologic model structure and parameterization and GCM structure and initial conditions. This was because it is challenging to address and compare uncertainties from all sources. Nevertheless, the five GCMs used herein cover the entire range of global mean precipitation and GMT of 19 GCMs from Coupled Model Inter-comparisons Project Five (CMIP5) reasonably well for 2020–2050 and RCP2.6 and RCP4.5 (Fig. S1). Moreover, 60 to 90% of the full range of future projections of 36 CMIP5 GCMs was captured by the five-model subset used for temperature and 40 to 80% of the full range of future projections for precipitation in the two catchments (from Fig. 1 in McSweeney and Jones 2016). This information provides a useful context for interpreting the results and may facilitate comparison of results across impact studies based on different ensemble subsets. Future studies should use multiple GCMs and different RCPs to examine the impacts of climate change or evaluate risk management measures.

Acknowledgements This study received support from the CMA Climate Change project (CCSF201722) and U.S.–China Clean Energy Research Center for Water–Energy Technologies project (2016YFE0102400). We acknowledge the Inter-Sectoral Impact Model Intercomparison Project, which provided climate data of the five GCMs, and the WATCH project, which provided climate forcing data of the hydrologic model from 1958 to 2001.

Open Access This article is distributed under the terms of the Creative Commons Attribution 4.0 International License (<http://creativecommons.org/licenses/by/4.0/>), which permits unrestricted use, distribution, and reproduction in any medium, provided you give appropriate credit to the original author(s) and the source, provide a link to the Creative Commons license, and indicate if changes were made.

References

- Bayliss A, Jones R (1992) The peaks-over-threshold database at the Institute of Hydrology. Report to UK Ministry of Agriculture in partial duration series modeling of extremes related to the choice of the threshold values. *J Hydrol* 303:215–230

- Dai A, Qian T, Trenberth KE et al (2009) Changes in continental freshwater discharge from 1948 to 2004. *J Clim* 22(10):2773–2792
- Dankers R, Arnell NW, Clark DB et al (2014) First look at changes in flood hazard in the Inter-Sectoral Impact Model Intercomparison Project ensemble. *PNAS* 111(9):3257–3261
- Fan J, Jiang YA, Chen Y et al (2014) The critical rainfall calculation in Kaidu River based on HBV hydrological model. *Desert Oasis Meteorol*. 2014 8(6):31–35
- FAO (1995–2003) The digitized soil map of the world and derived soil properties (version 3.5), FAO land and water digital media series 1. FAO, Rome
- Fu JY, Jiang D, Huang YH (2014) Population grid_China. *Acta Geograph Sin* 69(Supplement):41–44 (in Chinese)
- Gao CY, Zhao QH, Liu Q (2016) Fractal characteristic of soil particle size under different vegetation types in riparian zone of the main stream of Beijiing River. *Res Soil Water Conserv* 23(2):37–42
- Gosling SN, Taylor RG, Arnell NW et al (2011) A comparative analysis of projected impacts of climate river runoff from global and catchment-scale hydrological models. *Hydrol Earth Syst Sci* 15:279–294
- Graham LP, Bergström S (2001) Water balance modeling in the Baltic Sea drainage basin—analysis of meteorological and hydrological approaches. *Meteorog Atmos Phys* 77:45–60
- Guo WN, Zhao WJ (2015) Variation characteristics of runoff in the Yiluo River. *Sout-to-North Water Diversion* 21:61–62 (in Chinese)
- Hao ZX, Zheng JY, Ge QS (2007) Precipitation cycles in the middle and lower Yellow River. *Acta Geograph Sin* 62(5):537–544 (in Chinese)
- He L, Chen WY (2003) An analysis of water regime in Beijiing’s lower reaches. *J Foshan Univ (Natural Science Edition)* 21(2):67–69 (in Chinese)
- He RM, Wang GQ, Zhang JY (2007) Impacts of environmental change on runoff in the Yiluohe River basin of the middle Yellow River. *Res Soil Water Conserv*, 2007 14(2):297–298 (301.in Chinese)
- Hempel S, Frieler K, Warszawski L et al (2013) A trend-preserving bias correction—the ISIMIP approach. *Earth Syst Discuss* (4):49–92
- Huang GR, Wu CH, Liu ZY et al (2015) Precipitation of extreme floods of the Feilaixia reservoir in the Beijiing River basin under climate change. *Adv Water Sci* 26(1):10–19 (in Chinese)
- IPCC (2013) Climate change 2013: the physical science basis. In: Stocker TF, Qin D, Plattner GK, Tignor M, Allen SK, Boschung J, Nauels A, Xia Y, Bex V, Midgley PM (eds) Contribution of working group I to the fifth assessment report of the intergovernmental panel on climate change. Cambridge University Press, Cambridge, pp 5,31,212,955
- IPCC (2014a) Summary for policymakers. In: Field CB, Barros VR, Dokken DJ, Mach KJ, Mastrandrea MD, Bilir TE, Chatterjee M, Ebi KL, Estrada YO, Genova RC, Girma B, Kissel ES, Levy AN, MacCracken S, Mastrandrea PR, White LL (eds) Climate change 2014: impact, adaptation, and vulnerability. Part A: Global and sectoral aspects. Contribution of working group II to the fifth assessment report of the intergovernmental panel on climate change. Cambridge University Press, Cambridge, p 14
- IPCC (2014b) Climate change 2014: impact, adaptation, and vulnerability. Part A: global and sectoral aspects. In: Field CB, Barros VR, Dokken DJ, Mach KJ, Mastrandrea MD, Bilir TE, Chatterjee M, Ebi KL, Estrada YO, Genova RC, Girma B, Kissel ES, Levy AN, MacCracken S, Mastrandrea PR, White LL (eds) Contribution of working group II to the fifth assessment report of the intergovernmental panel on climate change. Cambridge University Press, Cambridge, pp 241–251
- IPCC (2014c) Climate change 2014: Synthesis Report. In: Core writing team, Pachauri RK, Meyer LA (eds) Contribution of working groups I, II and III to the fifth assessment report of the intergovernmental panel on climate change. IPCC, Geneva, pp 56
- Kang ES, Cheng GD, Lan YC et al (2001) Alpine runoff simulation of the Yalong River for the south-north water diversion. *J Glaciol Geocryol* 23(1):139–148 (in Chinese)
- Kay A, Davies H, Bell V et al (2009) Comparison of uncertainty sources for climate change impacts: flood frequency in England. *Clim Chang* 92:41–63
- Krysanova V, Bronstert A, Müller-Wohlferl DI (1999) Modelling river discharge for large drainage basins: from lumped to distributed approach. *Hydrol Sci J* 44:313–333
- Li Y, Zhang PF (2014) Analysis of change characteristics and variability of runoff in Beijiing River basin under influence of human activity. *J Water Resour Water Eng* 25(2):61–65 (in Chinese)
- Li SH, Hu CH, Wang HL et al (2015) Pattern analysis on land use/cover changes in Yiluo drainage. *Meteorol Environ Sci* 38(1):108–113 (in Chinese)
- Lindström G, Johansson B, Persson M et al (1997) Development and test of the distributed HBV-96 hydrological model. *J Hydrol* 201:272–288
- Liu LL, Fischer T, Jiang T et al (2013a) Comparison of uncertainties in projected flood frequency of the Zhujiang River, South China. *Quat Int* 304(2):51–61

- Liu XM, Dai XQ, Zhong YD et al (2013b) Analysis of changes in the relationship between precipitation and streamflow in the Yiluo River, China. *Theor Appl Climatol* 114:183–191
- Lu WX, Liu BJ, Chen XH et al (2013) Characteristics of precipitation period in Pear River basin. *J China Hydrol* 33(2):82–86 (in Chinese)
- McSweeney CF, Jones RG (2016) How representative is the spread of climate projections from the 5 CMIP5 GCMs used in ISI-MIP? *Climate Serv* 1:24–29
- Meng YJ, Bai ML, Li XC, Yang J (2015) Applied analysis on flood critical areal rainfall over Xilamulun River basin based on HBV hydrological model. *Meteorol J Inner Mongolia* 4:14–17
- Nash JE, Sutcliffe J (1970) River flow forecasting through conceptual models part I—a discussion of principles. *J Hydrol* 10(3):282–290
- Saelthun, N.R. (1996) The Nordic HBV model. Description and documentation of the model version developed for the project climate change and energy production. NVE Publication 7, Norwegian Resources and Energy Administration, Oslo
- Schellnhuber HJ, Hare WL, Serdeczny O et al (2012) Turn down the heat: why a 4°C warmer world must be avoided. tech. Rep., commissioned by the World Bank, Washington, D.C
- Schewe J., Levermann A., Meinshausen M. (2011) Climate change under a scenario near 1.5°C of global warming: monsoon intensification, ocean warming and static sea level rise. *Earth Syst. Dynam*, 2(1): 25–35
- Schewe J, Heinke J, Gerten D et al (2014) Multimodel assessment of water scarcity under climate change. *PNAS* 111(9):3245–3250
- Schleussner CF, Kissner TK, Fischer EM et al (2016) Differential climate impacts for policy-relevant limits to global warming: the case of 1.5°C and 2°C. *Earth Syst Dynam* 7(2):327–351. <https://doi.org/10.5194/esd-7-327-2016>
- Shang YL, Wang DH, Li L (2004) Development and updation of national dataset at a scale of 1: 250 000. *Sci Surv Mapp* 29(7):92–95 (in Chinese)
- Su BD, Huang JL, Zeng XF et al (2017) Impacts of climate change on streamflow in upper Yangtze River basin. *Clim Chang* 141:533–546
- Todd MC, Taylor RG, Osborn TJ et al (2011) Uncertainty in climate change impacts on basin-scale freshwater resources—preface to the special issue: the QUEST-GSI methodology and synthesis of results. *Hydrol Earth Syst Sci* 15:1035–1046
- UNFCCC (2010) FCCC/CP/2010/7/Add.1: Decision 1/CP.16, The Cancun Agreements. UNFCCC Cancun, pp 1–31
- UNFCCC (2015) FCCC/CP/2015/L.9/Rev.1: Adoption of the Paris agreement. UNFCCC, Paris, pp 1–32
- Wang GM (2014) Analysis on rain-rainoff in dry season of Beijiang River basin. *Guandong Water Resour Hydropower* 7:65–75 (in Chinese)
- Wang WT, Qian LX (2012) Spatial distribution and seasonal variation of evapotranspiration in Yiluo River basin on MODIS data. *Resour Sci* 34(8):1582–1590 (in Chinese)
- Wang Y, Ding YJ, Ye BS et al (2013) Contributions of climate and human activities to changes in runoff of the Yellow and Yangtze rivers from 1950 to 2008. *Sci Chin: Earth Sci* 56(8):1398–1412
- Warszawski L, Frieler K, Huber V et al (2014) The Inter-Sectoral Impact Model Intercomparison project (ISI-MIP): project framework. *PNAS* 111(9):3228–3232
- Weedon GP, Gomes S, Viterbo P et al (2010) The WATCH forcing data 1958–2001: a meteorological forcing dataset for land surface- and hydrological-models. WATCH Technical Report No.22, pp 1–41. Available at www.eu-watch.org
- Weedon GP, Balsamo G, Bellouin N et al (2014) The WFDEI meteorological forcing data set: WATCH forcing data methodology applied to ERA-interim reanalysis data. *Water Resour Res* 50(9):7505–7514
- Wu ZY, Lu GH, Liu ZY et al (2013) Trends of extreme flood events in the Pearl River basin during 1951–2010. *Adv Clim Chang Res* 4(2):110–116
- Xu ZX (2009) Hydrological models. Science Press, Beijing
- You DW, Tang CL, Deng S (2006) The early atmosphere-ocean characteristics for discharge abnormality of Xijiang and Beijiang River in winter. *Guandong Meteorol* 1:18–21 (in Chinese)
- Zha ZX, Wu MH, Ren XY (2001) Dataset of national land-use at a scale of 1:500 000. *Land Resour Informatization* 2:17–21 (in Chinese)
- Zhang YJ, Wu H, Wu SA, Chen SB (2014) Determination of area precipitation thresholds of rainstorm-flood hazard in the Nandu River basin. *J Appl Meteorol Sci* 25:731–740 (in Chinese)
- Zhao WM, Wang QZ, Liu XW et al (2006) Research on runoff generation in typical hydrological drainages in the Yellow River. Yellow River Conservancy Press, Zhengzhou (in Chinese)
- Zhao YZ, Zhang JX, Zhang SA et al (2007) Application of HBV model in Guanzhai catchment of the Huaihe River. *J Chin hydrolo* 27(2):57–59 6. (in Chinese)
- Zhao HY, Zhang YL, Wang ZW et al (2015) Threshold of precipitation for Qinhe River basin flood based on HBV model. *Res Soil Water Conserv* 22(5):74–48 (in Chinese)